



CrossMark
 click for updates

Cite this: *RSC Adv.*, 2015, 5, 34557

Cyclodextrin-tunable reversible self-assembly of a thermoresponsive Y-shaped polymer†

Hao Yao,^a Wei Tian,^{*a} Yuezhou Liu,^a Yang Bai,^b Dizheng Liu,^a Tingting Liu,^a Miao Qi,^a Min Wang^a and Yuyang Liu^a

Tuning the reversible self-assembly process of stimuli-responsive topological polymers in solution has theoretical and practical significance. In this study, we covalently incorporated β -cyclodextrin (β -CD) onto a thermoresponsive Y-shaped polymer to investigate the influence of β -CD on the morphology, size and reversibility of self-assemblies. Transmission electron microscopy, atomic force microscopy, and dynamic light scattering results indicated that the morphology and size of the polymer self-assemblies present a good reversibility during the whole heating-cooling process. The self-assembly morphology gradually changed from dot-like micelles to noticeable core-corona-structured micelles, and finally back to dot-like micelles again. Meantime, the size of self-assemblies first increased from several tens of nanometers to hundreds of nanometers, and then decreased to get close to the initial value. The attached β -CD units have a pronounced regulation effect on the reversible self-assembly process. The corresponding mechanism is attributed to the abilities of β -CD itself to conduct inclusion complexation, induce intermolecular hydrogen bonding interaction and present steric hindrance. Our study has expanded a new idea to reversibly tune the morphology and size of stimulus-responsive topological polymer self-assemblies.

Received 17th February 2015
 Accepted 8th April 2015

DOI: 10.1039/c5ra03064a

www.rsc.org/advances

Introduction

Y-shaped polymers belong to an important category of nonlinear miktoarm star copolymers that exhibit unique morphologies and phase behaviors.^{1–11} On the other hand, stimulus-responsive polymers can be crafted into new smart materials because of the responsive abilities to temperature, pH, light, electrolytes, mechanical stress, *etc.*¹² By combining with the above-mentioned two kinds of special polymers, stimulus-responsive Y-shaped polymers have been designed and considerable focus has been given to the self-assembly investigations in aqueous media due to their potential applications in biological medicine.^{13–19} For instance, Liu's group reported the synthesis of a variety of stimulus-responsive Y-shaped polymers and the diverse micellization when subjected to changes of external environment, such as temperature, pH or both of them.⁷ More importantly, it is necessary to regulate the morphology, size and reversibility of stimulus-responsive self-assemblies for further expanding their

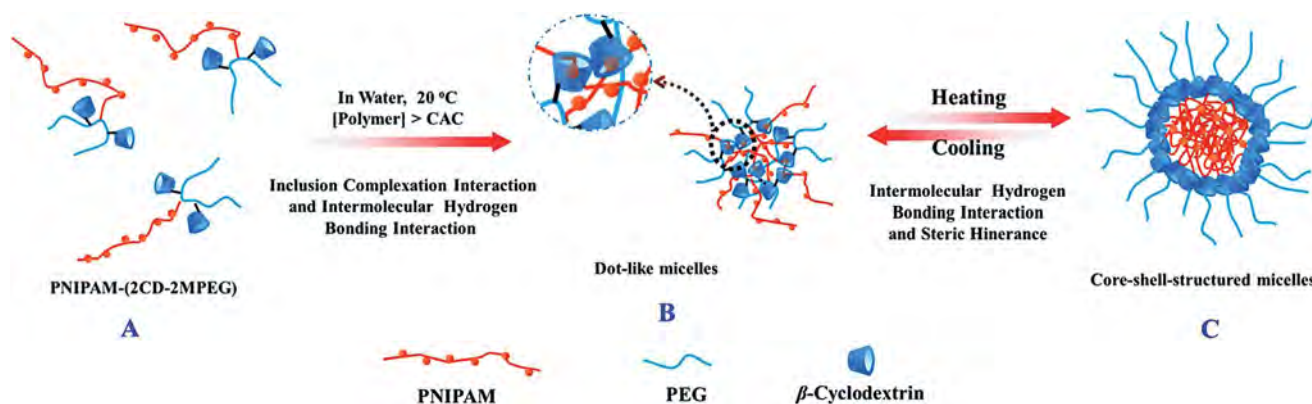
applications.⁸ As we know, however, the reversibility and tunable mechanism of these self-assemblies has been little studied yet.

For this purpose, we put the sight to cyclodextrins (CDs), which possess a hydrophobic cavity that can bind various guest molecules.^{20,21} In recent years, CDs have been extensively studied as convenient building blocks to construct polymeric nano-assemblies. For example, Yuan's group described voltage or light responsive block copolymers *via* β -CD/ferroence or α -CD/azobenzene complexation that can reversibly self-assemble and disassemble when responding to voltage or light.²² Moreover, CDs were also utilized to regulate the self-assembly behaviors of topological polymers.^{23–25} Jiang's group prepared a giant multiarm polymer terminated by β -CD, and further assembled into nanoparticles *via* the β -CD/adamantane inclusion complex.²⁴ Li group utilized the host-guest interaction of β -CD and adamantane to tune the self-assembled morphology of amphiphilic star-block copolymers from nanogel-like large compound micelles transformed into vesicular nanostructures.²⁵ To the best of our knowledge, however, when the CD complexations are subjected to external stimuli, such as variations in pH,²⁶ redox reagents,²⁷ and exposure to UV rays,²⁸ they may disassociate. Particularly, the CD complexations are more susceptible to the change of temperature because the association constant of the complexation is intrinsically related to the temperature mostly.²⁹ Thus, it is intractable to regulate the reversibility of stimulus-responsive

^aThe Key Laboratory of Space Applied Physics and Chemistry, Ministry of Education and Shaanxi Key Laboratory of Macromolecular Science and Technology, School of Science, Northwestern Polytechnical University, Xi'an, 710072, P. R. China. E-mail: happytw_3000@nwpu.edu.cn

^bXi'an Modern Chemistry Research Institute, Xi'an, 710065, P. R. China

† Electronic supplementary information (ESI) available: Synthesis, characterization of PNIPAM-(2CD-2MPEG). See DOI: 10.1039/c5ra03064a



Scheme 1 Schematic representation for the possible reversible self-assembly mechanism of PNIPAM-(2CD-2MPEG) in aqueous solution. (A) Chemical structure model of PNIPAM-(2CD-2MPEG); (A-B) PNIPAM-(2CD-2MPEG) molecules first self-assemble into dot-like micelles at 20 °C driven by the inclusion complexation interaction between the cavities of β-CD and isopropyl group of PNIPAM as well as the intermolecular hydrogen bonding interaction; (B-C-B) the reversible self-assembly behavior of PNIPAM-(2CD-2MPEG) can be effectively tuned during the heating-cooling process based on the intermolecular hydrogen bonding interaction and steric hindrance of β-CD.

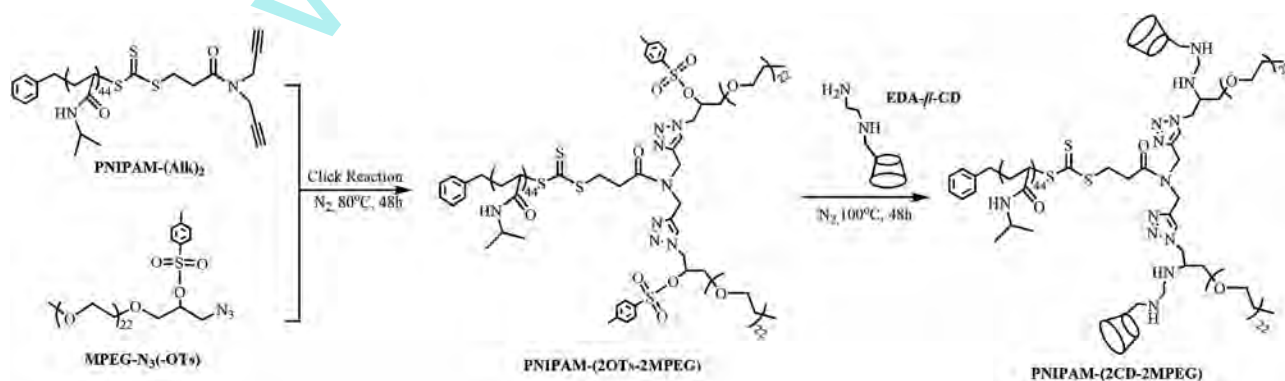
Y-shaped polymer self-assemblies *via* the conventional supramolecular complexation between CD and guest molecules.

On the basis of the consideration above, we expect to incorporate β-CD onto the thermo-responsive Y-shaped polymer by covalent bond, and aim to investigate the effect of covalently linked β-CD on the reversible self-assembly process of this kind of topological polymer. In our previous work,³⁰ we have incorporated β-CD units into the branching points of hyperbranched polymer, and focused on its synthesis and encapsulation behavior. Nevertheless, the effect of covalently linked β-CD on the reversible self-assembly behavior of stimulus-responsive Y-shaped polymers has rarely been reported in the literature thus far. Herein, a Y-shaped polymer with one temperature-sensitive poly(*N*-isopropylacrylamide) (PNIPAM) arm and two hydrophilic methoxypolyethylene glycol (MPEG) arms bearing two β-CD units adjacent to the branching points (PNIPAM-(2CD-2MPEG)) was first synthesized. The thermo-triggered self-assembly behavior of PNIPAM-(2CD-2MPEG) in aqueous solution was then investigated in detail. During the heating-cooling process, the morphology and size of formed self-assemblies present a good reversibility. The attached β-CD units have a pronounced influence on the reversible self-assembly process

due to the existences of the inclusion complexation interaction, intermolecular hydrogen bonding interaction and steric hindrance (Scheme 1).

Results and discussion

To study the influence of β-CD on the self-assembly of the final Y-shaped polymer, PNIPAM-(2CD-2MPEG) was synthesized according to the routes as shown in Scheme 2. Firstly, PNIPAM bearing two alkynyl groups (PNIPAM- Alk_2) was prepared by reversible addition-fragmentation chain transfer polymerization (RAFT) using the dipropargyl-terminated RAFT agent (CTA- Alk_2), which was synthesized by traditional amidation reaction (Scheme S1†). Simultaneously, MPEG containing an azido group and a tolylsulfonyl group at the same chain-end (MMPEG- $\text{N}_3(-\text{OTs})$) was synthesized *via* sequentially terminal modifications (Scheme S2†). With the above end-functional polymers, the Y-shaped polymer precursor (PNIPAM-(2OTs-2MPEG)) was then synthesized *via* the click reaction (Scheme 2). All above products were well-defined characterized by ^1H and ^{13}C NMRs, FTIR, electrospray ionization mass spectrometry and size exclusion chromatography/multiangle laser light scattering



Scheme 2 Synthetic routes for PNIPAM-(2CD-2MPEG).

(SEC-MALLS). The characterization data and corresponding spectra were provided in the ESI (Fig. S1–S11†). Finally, PNIPAM-(2CD-2MPEG) was obtained *via* nucleophilic substitution reaction between PNIPAM-(2OTs-2MPEG) and an excess of ethylenediamine β -CD (EDA- β -CD) (Scheme 2).

In the ^1H and ^{13}C NMR spectra of PNIPAM-(2CD-2MPEG) (Fig. S9III and S10III†), the characteristic signals of β -CD can be observed at $\delta = 4.4, 4.8$ and $5.5\text{--}6.0$ for protons of 6-OH, 1-H and 2, 3-OH as well as $\delta = 72\text{--}73$ for carbons of C-2, 3 and 5 positions compared to ^1H and ^{13}C NMR spectra of PNIPAM-(2OTs-2MPEG), respectively. The integral ratio of peak *k* (methine protons of PNIPAM side chain) to peak 1-H (protons at C-1 position of β -CD) was calculated to be 1.92 (Fig. S9III†). This means that the β -CD number of per PNIPAM-(2CD-2MPEG) molecule was close to 2, which is in accordance with the expected structure. Furthermore, SEC/MALLS results show that the M_n increased from 10 000 for PNIPAM-(2OTs-2MPEG) to 12 100 for PNIPAM-(2CD-2MPEG), with an increment of 2100 approximately equal to two β -CD units (Table S2†), which further confirmed the successful synthesis of the final Y-shaped polymer.

With the final product PNIPAM-(2CD-2MPEG), its self-assembly process was easily promoted *via* directly dissolving in water with a concentration of 1 mg mL^{-1} . Transmission electron microscopy (TEM), atomic force microscopy (AFM), dynamic/static light scattering (DLS/SLS), fluorescence spectrophotometry (FL), zeta-potentials, ^1H NMR (in D_2O), 2D NOSEY NMR, and ATR-FTIR measurements were conducted to obtain deeper insight into the morphology and size of self-assemblies. Particularly, the reversibility and corresponding β -CD-tunable mechanism of PNIPAM-(2CD-2MPEG) self-assemblies were well-defined investigated as the key point of this work.

TEM and AFM were first used to visualize the morphology and size of self-assemblies from PNIPAM-(2CD-2MPEG). Typical TEM images of PNIPAM-(2CD-2MPEG) aqueous solutions were obtained by drying aqueous solutions of samples at various temperatures on a copper grid without staining (Fig. 1). Significant differences on the self-assembly behavior caused by the covalently incorporated β -CD units were observed during the heating-cooling process. At initial $20\text{ }^\circ\text{C}$, dot-like micelles with around 20 nm in average diameter ($D_{\text{av,TEM}}$) were found in PNIPAM-(2CD-2MPEG) aqueous solution (Fig. 1A and F). When the solution temperature increased to $60\text{ }^\circ\text{C}$, the self-assembly morphology gradually transferred from solid spherical micelles to evidently core-corona-structured micelles with a $D_{\text{av,TEM}}$ value of 175 nm (Fig. 1C and H). On the contrary, no significant self-assembly morphology was observed as seen from the TEM image of PNIPAM-(2OTs-2MPEG) without β -CD aqueous solution at $20\text{ }^\circ\text{C}$ (Fig. S12A†). As the PNIPAM-(2OTs-2MPEG) solution temperature was increased to $60\text{ }^\circ\text{C}$, the solid spherical micelles were found with a $D_{\text{av,TEM}}$ value of 287 nm (Fig. S12B†), which was bigger than those of core-corona-structured micelles based on PNIPAM-(2CD-2MPEG). Furthermore, the micellar solution of PNIPAM-(2CD-2MPEG) during the heating-cooling process was confirmed to present a good reversibility. With the solution temperature decreasing to $20\text{ }^\circ\text{C}$,

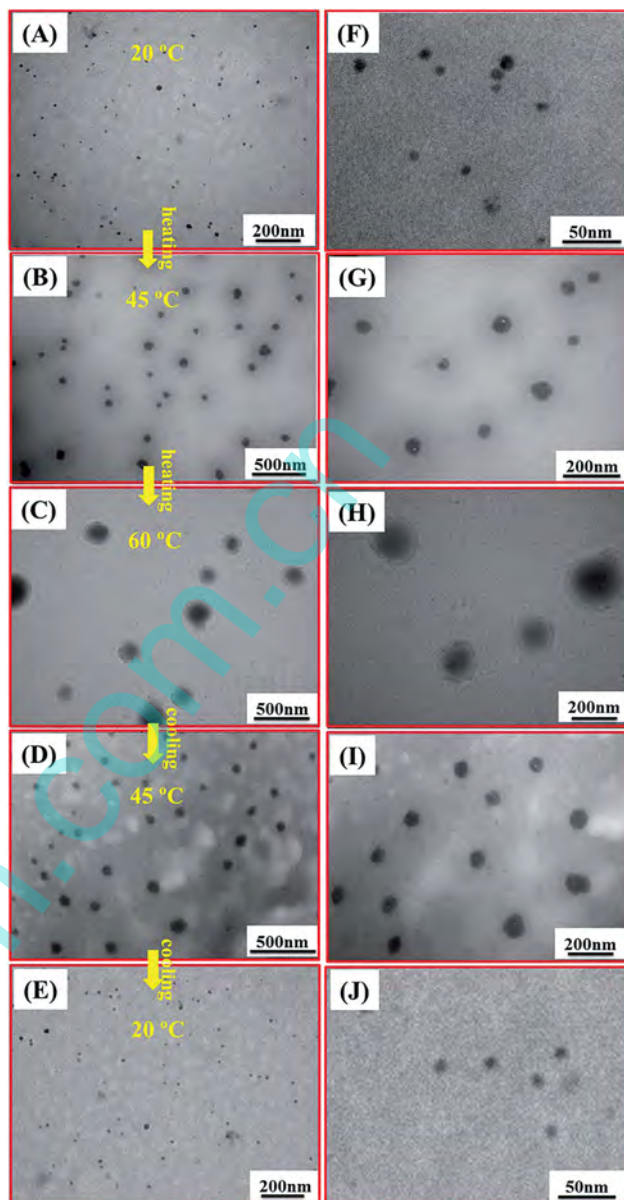


Fig. 1 Typical TEM images of PNIPAM-(2CD-2MPEG) aqueous solutions (A–E) with a concentration of 1.0 mg mL^{-1} during the heating-cooling process; (F–J) typical magnification images of A–E.

the self-assembly morphology gradually transferred to dot-like micelles again (Fig. 1E and J) and the $D_{\text{av,TEM}}$ value of micelles also went back to about 20 nm . Additionally, the reason for huge differences the chain length and the size observed by TEM could be attributed to the coupling of many small micelles when the solution was heated according to the literatures.^{31,32} Correspondingly, the AFM images of PNIPAM-(2CD-2MPEG) aqueous solutions were obtained to further verify the formation of the self-assemblies (Fig. 2). Regular dot-like self-assembly morphology at $20\text{ }^\circ\text{C}$ was observed in Fig. 2A. Further heating to $60\text{ }^\circ\text{C}$, thermo-triggered bigger spherical micelles were observed in Fig. 2B. Furthermore, the self-assembly morphology recovered initial state as the solution temperature went back to $20\text{ }^\circ\text{C}$ (Fig. 2C), indicating a reversible self-assembly process.

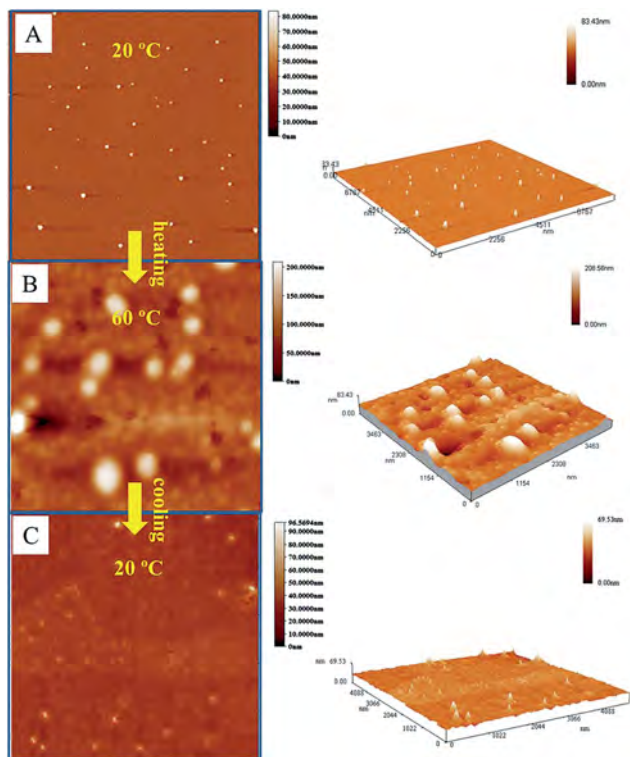


Fig. 2 Typical AFM images of PNIPAM-(2CD-2MPEG) aqueous solutions (A–C) with a concentration of 1.0 mg mL^{-1} during the heating-cooling process.

Thus, the results of AFM were in agreement with the results of TEM.

Furthermore, the hydrodynamic diameter (D_h) and the diameter distribution of PNIPAM-(2CD-2MPEG) self-assemblies were determined by DLS as shown in Table 1 and Fig. 3. DLS analysis shows a similar reversible self-assembly process compared to the results of TEM and AFM. As can be seen from Fig. 3A, the D_h value of self-assemblies at initial 20°C is 29 nm, which was considered as the self-assembled nanostructure, rather than a polymer chain. The D_h value then increased to 269 nm at 60°C , whereas became to 31 nm as the solution was cooled to 20°C . It should be noted that the D_h values of these self-assemblies are larger than those of $D_{\text{av,TEM}}$ values determined by TEM images (Table 1). The reason for this discrepancy may be attributed to the collapse or shrinkage of the micelles during the preparation of TEM samples.

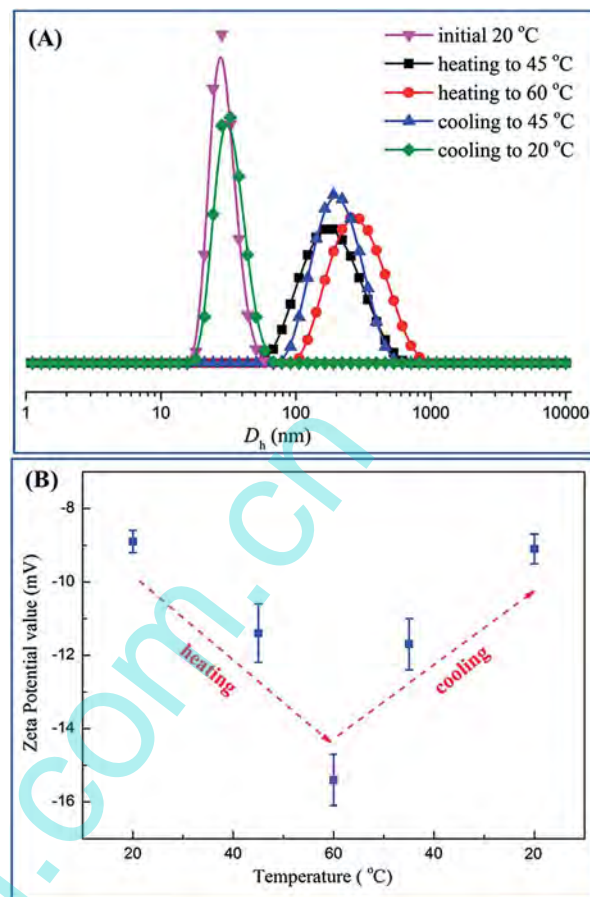


Fig. 3 DLS results: D_h of PNIPAM-(2CD-2MPEG) (A) and the change tendency of zeta potential value (B) in aqueous solution at various temperatures. [Polymer] = 1 mg mL^{-1} .

Additionally, the reversibility of self-assembly process was also proved by the PDI and the zeta potential measurements (Fig. 3B and Table 1). With the temperature heating from 20°C to 60°C and cooling to 20°C , the PDI value was 0.646, 0.177, 0.503 and the zeta potential value was -8.9 , -15.4 , -9.1 indicating a good reversibility. To further confirm this point, we utilized a combination of SLS and DLS techniques to discriminate the inner structure of self-assemblies at 20°C (including initial and final states). According to literature, the R_g/R_h value can predict the particle morphology. For hard spheres, the theoretical value is 0.77, while for vesicles, the value is 1.0.³³ The R_g/R_h values of

Table 1 DLS results of PNIPAM-(2CD-2MPEG) self-assemblies in aqueous solutions (1 mg mL^{-1}) during the heating-cooling process

T ($^\circ\text{C}$)	$D_{\text{av,TEM}}^a$ (nm)	$D_{\text{h,DLS}}^b$ (nm)	PDI ^c	Zeta potential value ^d (mV)
20	20	29	0.646	-8.9
45 (Heating)	72	172	0.127	-11.4
60 (Heating)	175	269	0.177	-15.4
45 (Cooling)	84	187	0.132	-11.7
20 (Cooling)	20	33	0.503	-9.1

^a Average diameter determined by TEM. ^b Hydrodynamic diameter determined by DLS. ^c Polydispersity of particles diameter determined by DLS. ^d Zeta potential value determined by DLS.

self-assemblies formed by PNIPAM-(2CD-2MPEG) at initial and final states are close to each other (0.92 and 0.87, respectively), indicating a similar inner structure of these self-assemblies.

In addition, the result implied that these self-assemblies are close to vesicular structure at 20 °C. The reason may be that the core of these self-assemblies still exhibits a certain hydration with water molecules. It may have a loose core being in accordance with the result from Ma's group.³⁴ A combination of TEM, AFM and SLS/DLS results indicated that the reversible self-assembly morphology and size of PNIPAM-(2CD-2MPEG) aqueous solutions during the heating-cooling process, which may be attributed to the covalently connected β -CD units.

Critical aggregation concentration (CAC), which acts as a key parameter to quantitatively confirm whether the aggregations have been formed, was estimated by FL using pyrene as a hydrophobic probe.³⁵ The ratio of the intensity of the first and third peaks (I_1/I_3) in the emission spectrum is very sensitive to the polarity of the medium surrounding pyrene molecules. Thus, the I_1/I_3 values of the pyrene emission spectra *versus* the logarithm of the PNIPAM-(2CD-2MPEG) concentration are shown in Fig. 4. The closed CAC values at an initial 20 °C (about 0.4291 mg mL⁻¹) and a final 20 °C (about 0.3157 mg mL⁻¹) were obtained from the intersection of the baseline and the tangent

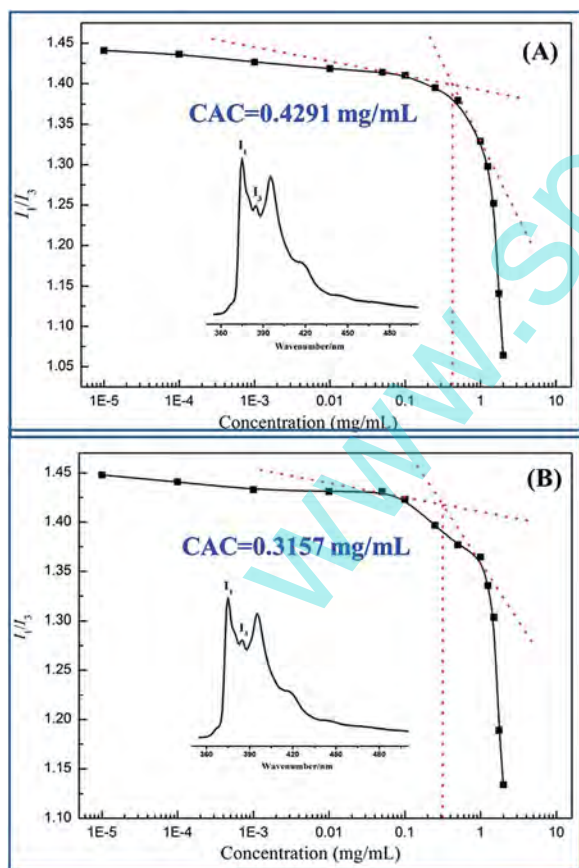


Fig. 4 Relationship between the fluorescence intensity ratio (I_1/I_3) and PNIPAM-(2CD-2MPEG) concentration in aqueous solutions at an initial 20 °C (A) and a final 20 °C (B) (inset: the pyrene fluorescence emission spectrum).

of the rapidly rising I_1/I_3 curves, indicating the formation of self-assemblies and good reversibility.

The core-corona structure of PNIPAM-(2CD-2MPEG) self-assemblies during the heating-cooling process was further confirmed by ¹H NMR analysis in D₂O and zeta-potential. ¹H NMR spectra of PNIPAM-(2CD-2MPEG) are shown in Fig. 5. When the solution temperature was gradually heated from 20 °C to 60 °C in D₂O, signals corresponding to PNIPAM segments dramatically weakened and shifted to downfield while MPEG segments only shifted but not faded. This suggested that PNIPAM segments collapsed into the micellar core after the lower critical solution temperature (LCST) transition (Fig. S15[†]), whereas MPEG segments formed the corona layer. Furthermore, when cooling the solution to 20 °C, the signals of PNIPAM segments restored gradually. This result also verified the decent reversibility of the self-assembly process. More importantly, the proton peak of 1-H in β -CD molecule was found to be shifted but not faded in D₂O NMR during the heating-cooling process (see enlarged part of Fig. 5). It suggested that β -CD units might be located on the corona layer of the micelles during the self-assembly process. Further evidence could be obtained by the zeta-potential analysis using 1-adamantane acid sodium (Ada-COONa) as guest molecule. Upon the addition of Ada-COONa into PNIPAM-(2CD-2MPEG) micellar solutions under the different conditions of initial 20 °C, heating to 60 °C and cooling to 20 °C (Table 2), all zeta-potential values are higher than those of samples without Ada-COONa. This means that β -CD units contributed to the hydrophilic corona layer during the self-assembly process according to the literature.³⁶

Based on the above results, we have preliminarily realized the influence of β -CD on the reversible self-assembly of PNIPAM-(2CD-2MPEG) in aqueous solution. Specifically, the attachment of β -CD units induces the formation of dot-like micelles at initial 20 °C. The possible reason may be attributed to the inclusion complexation interactions between the hydrophobic cavities of β -CD and isopropyl groups of PNIPAM chains. When rising solution temperature to 60 °C, the rigid β -CD units with steric hindrance efficiently inhibit the coalescence of the self-assemblies during the thermo-triggered process, leading to a relatively smaller size and noticeable core-corona structure, as compared to PNIPAM-(2OTs-2MPEG) precursor solution without β -CD units (Fig. S12B[†]). The self-assembly morphology and size then recover the initial state as temperature went back to 20 °C caused by the same driving force with the initial 20 °C, that's the inclusion complexation interactions. During the whole heating-cooling process, the intermolecular hydrogen bonding interactions of β -CD and PNIPAM segments play an important role in holding the stability of self-assemblies. This possible reversible self-assembly mechanism of PNIPAM-(2CD-2MPEG) in aqueous solution is illustrated in Scheme 1.

The above β -CD-tunable reversible self-assembly mechanism can be further confirmed by 2D NOESY NMR and ATR-FTIR experiments. At initial 20 °C, the inclusion complexation interactions between β -CD and isopropyl groups of PNIPAM segments was proved by 2D NOESY NMR experiments, which has been widely adopted by many researchers to confirm the

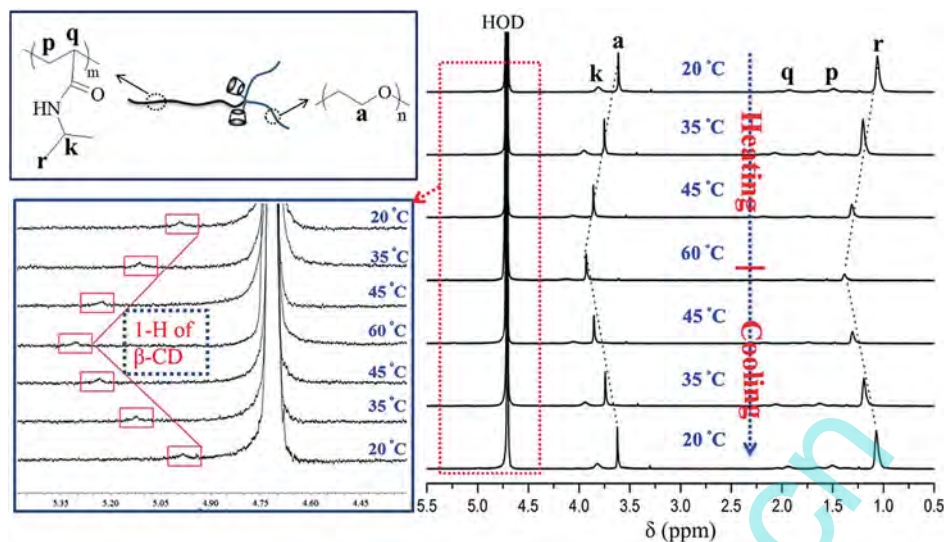


Fig. 5 ^1H NMR spectra of PNIPAM-(2CD-2MPEG) (1.0 mg mL^{-1}) in D_2O at various temperatures.

Table 2 Zeta-potential values of PNIPAM-(2CD-2MPEG) without and with Ada-COONa (1 mg mL^{-1}) at $20 \text{ }^\circ\text{C}$, $60 \text{ }^\circ\text{C}$ and $20 \text{ }^\circ\text{C}$ (cooling)

Zeta potential value (mV)	$20 \text{ }^\circ\text{C}$	$60 \text{ }^\circ\text{C}$	$20 \text{ }^\circ\text{C}$ (cooling)
PNIPAM-(2CD-2MPEG) solutions	-8.9	-15.4	-9.1
PNIPAM-(2CD-2MPEG) solutions with Ada-COONa	-17.4	-19.2	-16.9

interaction between CDs and guest molecules.^{27,29,34} As displayed in Fig. 6, the 2D NOESY NMR spectra shows that the protons of isopropyl groups at about 1.05 ppm were directly correlated to the protons at $\delta = 3.4\text{--}3.6$ ppm which corresponded to 3-H and 5-H protons of $\beta\text{-CD}$. As reported by Ma's group³⁴ and Cho's group,³⁷ the inclusion complexation between CDs and isopropyl groups of PNIPAM chains could lead the formation of aggregations, and this interaction might serve as a physical cross-link to hold polymer chains together. Additionally, the association constant (K_a) between $\beta\text{-CD}$ and isopropyl

group is about 3.8 mmol dm^{-3} as determined by spectrophotometrically by Matsui and Mochida.³⁸ On the other aspect, to confirm the existence of hydrogen bonding in heating-cooling process, the ATR-FTIR spectra of PNIPAM-(2CD-2MPEG) in THF and H_2O were compared. As shown in Fig. 7, one significant change could be found in the absorbance peak of $\text{C}=\text{O}$ groups. Comparing the spectra of PNIPAM-(2CD-2MPEG) solutions in THF and H_2O at $20 \text{ }^\circ\text{C}$, respectively, the peaks at about 1650 cm^{-1} shifted to lower wavenumbers of 1640 cm^{-1} , along with the expanding and strengthening of $\text{C}=\text{O}$

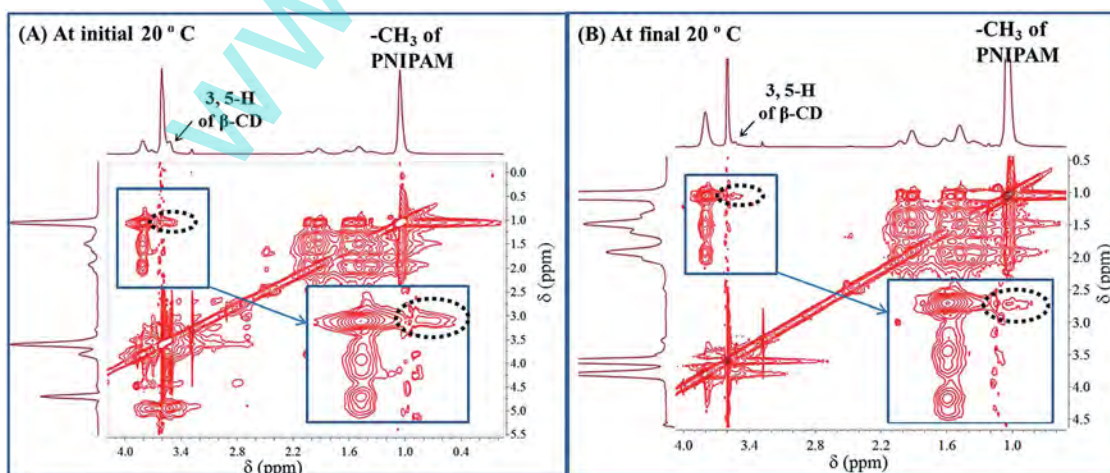


Fig. 6 2D NOESY NMR spectra of PNIPAM-(2CD-2MPEG) in D_2O at a concentration of 5 mg mL^{-1} at an initial $20 \text{ }^\circ\text{C}$ (A) and a final $20 \text{ }^\circ\text{C}$ (B), respectively.

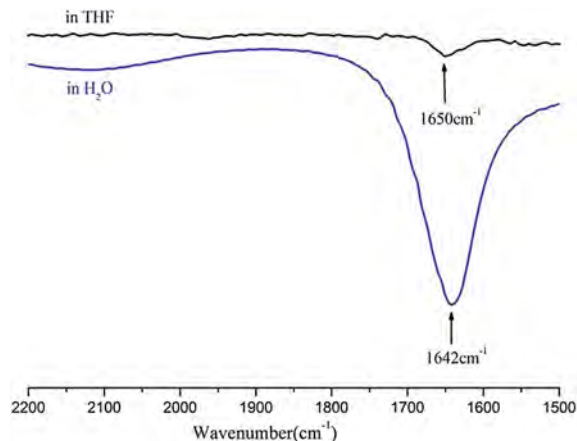


Fig. 7 ATR-FTIR spectra of PNIPAM-(2CD-2MPEG) in THF or H₂O at 20 °C with a concentration of 1.0 mg mL⁻¹.

absorbance. The formation of strong inter/intra-polymer hydrogen bonding contributes to the above obvious shifting in ATR-FTIR spectra. This result was in agreement with a report on the hydrogen bonding-mediated vesicular self-assembly by Ghosh's group.³⁹ Summarily, the above results further confirmed the rationality of the proposed β -CD-tunable reversible self-assembly mechanism of PNIPAM-(2CD-2MPEG) in aqueous solution.

Conclusions

The incorporation of covalently connected β -CD onto the thermoresponsive Y-shaped polymer can reversibly tune the morphology and size of the self-assemblies. During the heating-cooling process, the self-assembly morphology gradually transferred from dot-like micelles to noticeable core-corona-structured micelles, and finally back to dot-like micelles. The size of self-assemblies increased from 29 to 269 nm, and then decreased to 33 nm according to the results of DLS. A similar change tendency was also found in TEM experiments. The mechanism of the reversible self-assembly can be attributed to the synergistic effect of the inclusion complexation interaction, intermolecular hydrogen bonding interaction and steric hindrance of β -CD units. We believe that the effect of covalently connected β -CD on the reversible self-assembly behavior of stimulus-responsive topological polymers will extend more applications in controlled drug delivery and biomedicine.

Experimental section

Materials

Methoxypolyethylene glycol (MPEG, $M_n = 1000$ Da) was purchased from Aladdin and was dried by azeotropic distillation in the presence of toluene. 1,2-Ethanediamine- β -CD (EDA- β -CD) was synthesized according to the literature.⁴⁰ Pyrene (Alfa Aesar, 99%), *N*-isopropylacrylamide (NIPAM, 99%, Acros) were used as received. Sodium azide (NaN₃) (99%, Aldrich), tosyl chloride (TsCl) (99%), epichlorohydrin (98%), *N,N*-dicyclohexylcarbodiimide (DCC, 95%), ammonium chloride (99%) and

N-hydroxysuccinimide (NHS, 95%) were from Sinopharm Chemical Reagent Co., Ltd., Shanghai, China. *N,N*-Dimethylformamide (DMF) and CH₂Cl₂ were dried with a 3 Å grade molecular sieve before use. 2,2'-Azobis(2-methylpropionitrile) (AIBN; Fluka, 99%) was recrystallized twice from methanol.

Synthesis and characterization of PNIPAM-(2CD-2MPEG) are found in ESI†

Polymer structure characterization. Fourier Transform Infrared (FTIR) spectra were recorded on a Nicolet iS10 IR spectrometer (Nicolet USA), casting samples into thin films on KBr. Transition mode was used and the wavenumber range was set from 4000 cm⁻¹ to 500 cm⁻¹. ATR-FTIR spectra of samples at various temperatures were processed by ATR correction. A solution of the sample in either THF or H₂O was placed in the liquid cell, and the spectra of the solutions were recorded. ¹H NMR and ¹³C NMR spectra were conducted on a Bruker Avance 300 spectrometer (Bruker BioSpin, Switzerland) operating at 300 MHz (¹H) in CDCl₃, DMSO-d₆ or D₂O. Electrospray ionization mass spectrometry was recorded using a microTOF-QII 10280 (Varian Inc., USA). The molecular structure parameters of the resulting polymers were determined on a DAWN EOS size exclusion chromatography/multiangle laser light scattering (SEC/MALLS). HPLC grade DMF containing LiCl (0.01 mol L⁻¹) (at 40 °C) or THF (at 25 °C) was used as eluent at a flow rate of 0.5 mL min⁻¹. The chromatographic system consisted of a Waters 515 pump, differential refractometer (Optilab rEX), and one-column MZ 10³ Å 300 × 8.0 mm for the DMF system as well as two-column MZ 10³ Å and 10⁴ Å for the THF system. The MALLS detector (DAWN EOS), quasi-elastic light scattering (QELS), and differential viscosity meter (ViscoStar) were placed between the SEC and the refractive index detector. The molecular weight (M_w) and molecular weight distribution (MWD) were determined using a SEC/DAWN EOS/Optilab rEX/QELS model. ASTRA software (Version 5.1.3.0) was utilized for acquisition and analysis of data.

Polymer solution characterization. TEM observations were conducted on a Hitachi H-7650 electron microscope at an acceleration voltage of 70 kV. Samples were prepared by dropping 10 μ L of micellar solution on copper grids without staining and then liquid nitrogen quenching cold, vacuum freeze-drying. Heating or cooling speed was kept at 20 °C min⁻¹, and then micellar solution was stable at a predetermined temperature for 5 min. The morphology was visualized using AFM with tapping mode and a Nanowizard II controller (Benyuan, CSPM 5500, China). Tip information: radius ≤ 10 nm, cantilever length 100 μ m, width 30 μ m, thickness 10 μ m, resonant frequency 300 kHz, and force constant 40 N m⁻¹. Samples were prepared by dropping 20 μ L of micellar solution onto freshly mica plates and then vacuum drying at 20 °C or 60 °C. All the images were acquired under a tapping mode. The size and size distribution of the aggregates at various temperatures were determined by dynamic light scattering (DLS) using a Malvern Zetasizer Nano ZS instrument. The polymer solutions (1 mg mL⁻¹) were passed through a 0.45 μ m microfilter and kept at a predetermined

temperature for 5 min before measurement. The scattered light of a vertically polarized He–Ne laser (633 nm) was measured at an angle of 173° and collected on an autocorrelator. SLS analysis was performed on a DAWN HELEOS-II multi-angle light scattering detector (Wyatt Technology Corporation, USA) operated at 665 nm, using gallium–arsenic as the incident laser beam source. SLS data were collected at 6 different concentrations of the aggregates and 18 different angles for each concentration. The data were analyzed using the Zimm plot method on HELEOS-II Firmware 2.4.0.4 advanced software to determine R_g .

Polymer solution properties. The critical aggregation concentration (CAC) of polymers was determined by fluorescence spectroscopy (Hitachi F-4600). The emission spectra of micellar solutions with a polymer concentration range from 1 to 1×10^{-4} mg mL⁻¹ and a fixed pyrene concentration of 6×10^{-6} M were recorded from 355 to 550 nm with an excitation wavelength of 335 nm. The emission intensity ratio of the first vibronic band to the third of the spectra (I_1/I_3 ratio) was calculated and plotted against the polymer concentration. The CAC was estimated as the cross-point when extrapolating the I_1/I_3 ratio at low and high concentration regions.

The LCST of the Y-shaped polymers were determined by UV-vis spectroscopy (Shimadzu UV-2550 model, Japan) first. The transmittance of the polymeric aqueous solutions (1 mg mL⁻¹) was recorded at temperature ranging from 25 to 50 °C. Sample cells were thermostated with an external constant temperature controller. The temperature ramp was set at 1 °C min⁻¹. Temperature corresponded to the onset of the decrease in transmittance was defined as LCST.

Acknowledgements

This work was supported by the National Science Foundations of China (no. 21374088). W.T. thanks the grant from the Program for New Century Excellent Talents of Ministry of Education (NCET-13-0476), the Key Laboratory Program of Science and Technology Coordinator Innovation Project of Shaanxi Province of China (2013SZS17-P01), the Program of New Staff and Research Area Project of NPU (13GH014602) and the Fundamental Research Funds for the Central Universities (3102015ZY096).

Notes and references

- 1 S. Peleshanko and V. V. Tsukruk, *Prog. Polym. Sci.*, 2008, **33**, 523–580.
- 2 Y. L. Cai and S. P. Armes, *Macromolecules*, 2005, **38**, 271–279.
- 3 Y. L. Cai, C. Burguiere and S. P. Armes, *Chem. Commun.*, 2004, 802.
- 4 Y. L. Cai, Y. Tang and S. P. Armes, *Macromolecules*, 2004, **37**, 9728–9737.
- 5 S. Peleshanko, J. Jeong, R. Gunawidjaja and V. V. Tsukruk, *Macromolecules*, 2004, **37**, 6511–6522.
- 6 S. Peleshanko, J. Jeong, V. V. Shevchenko, K. L. Genson, Y. Pikus, M. Ornatska, S. Petrash and V. V. Tsukruk, *Macromolecules*, 2004, **37**, 7497–7506.
- 7 (a) J. Y. Rao, Y. F. Zhang, J. Y. Zhang and S. Y. Liu, *Biomacromolecules*, 2008, **9**, 2586–2593; (b) H. Liu, J. Xu, J. L. Jiang, J. Yin, R. Narain, Y. L. Cai and S. Y. Liu, *J. Polym. Sci., Part A: Polym. Chem.*, 2007, **45**, 1446–1462.
- 8 (a) C. Feng, G. L. Lu, G. Sun, X. W. Liu and X. Y. Huang, *Polym. Chem.*, 2014, **5**, 6027; (b) X. Jiang, C. Feng, G. L. Lu and X. Y. Huang, *ACS Macro Lett.*, 2014, **3**, 1121.
- 9 J. Z. Du and Y. M. Chen, *Macromolecules*, 2004, **37**, 3588–3594.
- 10 H. H. Liu, K. Miao, G. D. Zhao, C. X. Li and Y. L. Zhao, *Polym. Chem.*, 2014, **5**, 3071.
- 11 K. Miao, H. H. Liu and Y. L. Zhao, *Polym. Chem.*, 2014, **5**, 3335.
- 12 F. Yuen and K. C. Tam, *Soft Matter*, 2010, **6**, 4613.
- 13 H. Xiong, P. Leonard and F. Seela, *Bioconjugate Chem.*, 2012, **23**, 856–870.
- 14 G. Maglio, F. Nicodemi, C. Conte, R. Palumbo, P. Tirino, E. Panza, A. Ianaro, F. Ungaro and F. Quaglia, *Biomacromolecules*, 2011, **12**, 4221–4229.
- 15 Y. Y. Li, X. Z. Zhang, H. Cheng, G. C. Kim, S. X. Cheng and R. X. Zhuo, *Biomacromolecules*, 2006, **7**, 2956–2960.
- 16 Y. Y. Li, X. Z. Zhang, G. C. Kim, H. Cheng, S. X. Cheng and R. X. Zhuo, *Small*, 2006, **2**, 917–923.
- 17 L. Y. Li, W. D. He, J. Li, B. Y. Zhang, T. T. Pan, X. L. Sun and Z. L. Ding, *Biomacromolecules*, 2010, **11**, 1882–1890.
- 18 A. V. Ambade, E. N. Savariar and S. Thayumanavan, *Mol. Pharm.*, 2005, **2**, 264–272.
- 19 F. Bensaid, O. T. D. Boullay, A. Amgoune, C. Pradel, L. H. Reddy, E. Didier, S. Sablé, G. Louit, D. Bazile and D. Bourissou, *Biomacromolecules*, 2013, **14**, 1189–1198.
- 20 Y. Kang, K. Guo, B. J. Li and S. Zhang, *Chem. Commun.*, 2014, **50**, 11083.
- 21 G. S. Chen and M. Jiang, *Chem. Soc. Rev.*, 2011, **40**, 2254.
- 22 (a) Q. Yan, R. Zhou, C. K. Fu, H. J. Zhang, Y. W. Yin and J. Y. Yuan, *Angew. Chem., Int. Ed.*, 2011, **50**, 4923–4927; (b) Q. Yan, Y. Xin, R. Zhou, Y. W. Yin and J. Y. Yuan, *Chem. Commun.*, 2011, **47**, 9594–9596.
- 23 C. Feng, G. L. Lu, Y. J. Li and X. Y. Huang, *Langmuir*, 2013, **29**, 10922.
- 24 J. J. Wang, J. L. Zhang, S. L. Yu, W. Wu and X. Q. Jiang, *ACS Macro Lett.*, 2013, **2**, 82–85.
- 25 J. L. Zhu, K. L. Liu, Z. X. Zhang, X. Z. Zhang and J. Li, *Chem. Commun.*, 2011, **47**, 12849.
- 26 Y. L. Zhao, Z. X. Li, S. Kabehie, Y. Y. Botros, J. F. Stoddart and J. I. Zink, *J. Am. Chem. Soc.*, 2010, **132**, 13016–13025.
- 27 Q. Yan, J. Y. Yuan, Z. N. Cai, Y. Xin, Y. Kang and Y. W. Yin, *J. Am. Chem. Soc.*, 2010, **132**, 9268–9270.
- 28 Y. Takashima, S. Hatanaka, M. Otsubo, M. Nakahata, T. Kakuta, A. Hashidzume, H. Yamaguchi and A. Harada, *Nat. Commun.*, 2012, **3**, 1270.
- 29 Z. Yang, X. D. Fan, W. Tian, D. Wang, H. T. Zhang and Y. Bai, *Langmuir*, 2014, **30**, 7319–7326.
- 30 W. Tian, X. Y. Wei, Y. Y. Liu and X. D. Fan, *Polym. Chem.*, 2013, **4**, 2850.
- 31 R. R. Taribagil, M. A. Hillmyer and T. P. Lodge, *Macromolecules*, 2010, **43**, 5396–5404.

- 32 V. Castelletto, I. W. Hamley, Y. Ma, X. Bories-Azeau, S. P. Armes and A. L. Lewis, *Langmuir*, 2004, **20**, 4306–4309.
- 33 J. Z. Du, H. Willcock, J. Patterson, I. Portman and R. O'Reilly, *Small*, 2011, **7**, 2070.
- 34 J. X. Zhang, K. Feng, M. Cuddihy, N. A. Kotov and P. X. Ma, *Soft Matter*, 2010, **6**, 610.
- 35 K. Kalyanasundaram and J. K. Thomas, *J. Am. Chem. Soc.*, 1977, **99**, 2039–2044.
- 36 Y. Bai, X. D. Fan, W. Tian, H. Yao, L. H. Zhuo, H. T. Zhang, W. W. Fan, Z. Yang and W. B. Zhang, *Polymer*, 2013, **54**, 3566–3573.
- 37 S. J. Han, M. K. Yoo, Y. K. Sung, Y. M. Lee and C. S. Cho, *Macromol. Rapid Commun.*, 1998, **19**, 403–407.
- 38 Y. Matsui and K. Mochida, *Bull. Chem. Soc. Jpn.*, 1979, **52**, 2808–2814.
- 39 M. R. Molla and S. Ghosh, *Chem.–Eur. J.*, 2012, **18**, 9860–9869.
- 40 Y. Liu, X. Fan and L. Gao, *Macromol. Biosci.*, 2003, **3**, 715–719.

www.spm.com.cn